Seismic critical-angle reflectometry: A method to characterize azimuthal anisotropy?

Martin Landrø[1,2] and Ilya Tsvankin[2]
[1] *Department of Petroleum Engineering and Applied Geophysics, NTNU, 7491 Trondheim, Norway*
[2] *Center for Wave Phenomena, Colorado School of Mines, Golden, Colorado, USA*

ABSTRACT

Existing anisotropic parameter-estimation algorithms that operate with long-offset data are based on the inversion of either nonhyperbolic moveout or wide-angle AVO response. Here, we show that valuable information about high-velocity anisotropic reservoirs can also be provided by the critical angle of reflected waves.

To explain the behavior of the critical angle, we develop weak-anisotropy approximations for vertical transverse isotropy and then use Tsvankin's notation to extend them to azimuthally anisotropic models of orthorhombic symmetry. The critical angle of P-waves in orthorhombic media strongly depends on the parameters $\epsilon^{(1)}$ and $\epsilon^{(2)}$ responsible for the symmetry-plane horizontal velocities in the high-velocity layer. The azimuthal variation of the critical angle for typical orthorhombic models can reach 6–7°, which translates into substantial changes in the critical offset of the reflected P-wave. The main diagnostic features of the critical-angle reflection employed in our method include the rapid increase of the reflection amplitude at the critical angle and the subsequent separation of the head wave.

Analysis of synthetic seismograms generated with the reflectivity method confirms that the azimuthal variation of the critical offset is detectable on wide-azimuth, long-spread data and can be qualitatively described by our linearized equations. However, this test also shows that estimation of the critical offset from the amplitude curve of the reflected wave is not straightforward. Additional complications may be caused by errors in computing the critical angle at the target from the measured critical offset and by the overburden noise train. Still, the azimuthally varying critical angle should help to constrain the dominant fracture directions in high-velocity reservoirs. Also, critical-angle reflectometry can be combined with other methods to reduce the uncertainty in anisotropic parameter estimates.

Key words: critical angle, wide-angle data, azimuthal anisotropy, transverse isotropy, amplitude variation with offset, reflection coefficient

1 INTRODUCTION

It is now widely accepted in the petroleum industry that most subsurface formations are anisotropic with respect to seismic wave propagation. Estimation of the relevant anisotropy parameters required to build reliable velocity models, however, remains a challenging and often ill-posed problem (e.g., Tsvankin, 2005; Tsvankin and Grechka, 2006). Long-offset reflection data play an important role in anisotropic velocity analysis because they are recorded for a wide range of angles with the vertical.

In particular, inversion of P-wave nonhyperbolic (long-spread) moveout for VTI (transversely isotropic

with a vertical symmetry axis) media is often used to estimate the anellipticity parameter η, which controls time processing of P-wave data (Alkhalifah and Tsvankin, 1995; Alkhalifah, 1997; Tsvankin, 2005). Nonhyperbolic moveout analysis has also been extended to more complicated, azimuthally anisotropic media composed of orthorhombic layers (Pech and Tsvankin, 2004; Vasconcelos and Tsvankin, 2004). However, despite a number of generally successful case studies (e.g., Toldi et al., 1999), nonhyperbolic moveout inversion is hampered by the trade-off between the normal-moveout (NMO) velocity and the quartic moveout coefficient. Even relatively low levels of correlated noise can create substantial uncertainty in the estimation of the parameter η in VTI media or the corresponding anellipticity parameters of orthorhombic media (Grechka and Tsvankin, 1998). On the whole, while nonhyperbolic moveout inversion can help in constraining velocity models for time processing, its application in reservoir characterization is much more problematic.

Another shortcoming of traveltime-inversion methods is their low vertical resolution, especially for relatively deep reservoirs. Higher resolution can be achieved by amplitude-varation-with-offset (AVO) analysis, which provides information about the local elastic properties at the reservoir level. For azimuthally anisotropic models that decribe naturally fractured reservoirs, the azimuthal variation of the AVO response is used to estimate the fracture orientation and identify areas of intense fracturing (Rüger, 2001; Gray et al., 2002; Hall and Kendall, 2003). Most existing AVO algorithms operate with the AVO gradient estimated from conventional-spread reflection data. Although including longer offsets significantly reduces the ambiguity of the amplitude inversion, especially for multicomponent data (Jílek, 2002), wide-angle AVO analysis is not yet common (Pankhurst et al., 2002). Even when the offset-to-depth ratio is sufficient to constrain the large-angle AVO terms, the low data quality and phase changes at long offsets cause serious complications for accurate amplitude picking.

Here, we suggest another way of employing long-offset data in anisotropic parameter estimation. The P-wave velocity in many hydrocarbon reservoirs is higher than that in the cap rock, which leads to critical and post-critical reflections in the recorded offset range. Landrø et al. (2004) proposed to measure the shift in the critical angle or offset observed on time-lapse data to monitor production in hydrocarbon reservoirs. If either the cap or reservoir layer is azimuthally anisotropic, the critical angle and the corresponding critical offset vary with azimuth. For 3D data with good coverage in azimuth and offset, the azimuthal variation of the critical angle can be used to identify the vertical symmetry planes of the model and constrain the anisotropy parameters. In contrast to AVO analysis, this method does not require accurate amplitude measurements for a wide range of offsets because the critical angle can be estimated from the point of the fastest amplitude increase.

We begin by briefly introducing ultrasonic critical-angle reflectometry based on laboratory measurements of the critical angle in various materials. Then we derive a concise weak-anisotropy approximation for the critical angle in VTI media and generalize this result for orthorhombic models often used to describe naturally fractured reservoirs. The analytic results help to identify the parameter combinations constrained by critical-angle measurements. To evaluate the feasibility of estimating the critical angle for orthorhombic media, we compute full-waveform synthetic seismograms using the reflectivity method. Finally, we discuss practical issues related to field-data application of the method.

2 ULTRASONIC CRITICAL-ANGLE REFLECTOMETRY

This paper extends to seismology the idea of the well-established method of ultrasonic measurements called "ultrasonic critical-angle reflectometry." The method is based on measuring the critical angle as function of azumuth in human bones, some composite materials, etc. (Antic and Mehta, 1997). The shift of the critical angle with azimuth is then inverted for the pertinent anisotropy parameters. Critical-angle reflectometry has become industry standard for a wide range of applications.

Although post-critical reflections are well-documented in seismological literature, implemetation of quantitative critical-angle reflectometry is not straightforward. First, many target horizons are located at significant depths and overlaid by a complex sequence of sedimentary layers. Multiple reflections and mode conversions in the overburden can create interference with the critical-angle event from the top or bottom of the reservoir. Second, the method requires a velocity increase at the target interface, which is not always the case for hydrocarbon reservoirs. Third, wide-azimuth data, which are needed to reconstruct the azimuthal variation of the critical angle, are routinely acquired only in OBC (ocean-bottom-cable) multicomponent surveys. Marine streamer data sets have narrow azimuthal coverage, while full-azimuth land data seldom include sufficiently long offsets.

Still, under favorable circumstances the critical angle can be detected on long-offset seismic data. Figure 1 displays a raw seismic gather that contains an interpretable reflection from an interface with a large positive velocity contrast. Despite the interference with noise and overburden events, this reflection can be identified for offsets up to about 4.5 km. The interfering arrivals can be suppressed by standard F-K filtering (Figure 2). Then, amplitude analysis can be used to identify the point of the fastest amplitude increase corresponding to

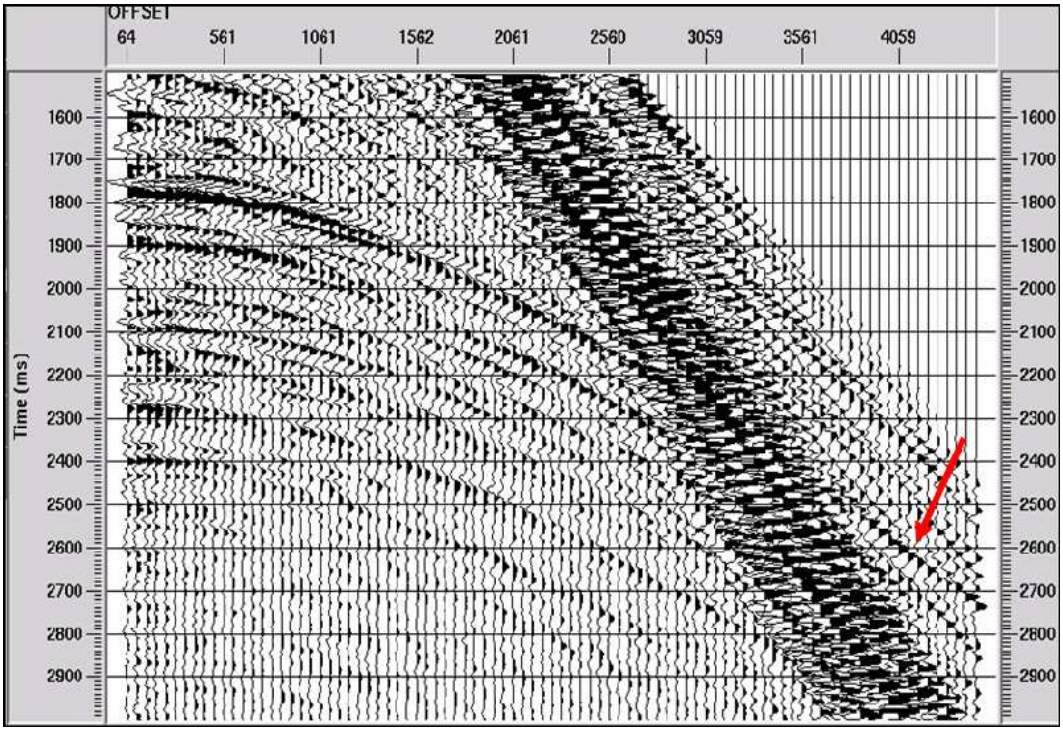

Figure 1. Common-receiver field gather of the vertical displacement component. The arrow marks a reflection from the top of a high-velocity layer.

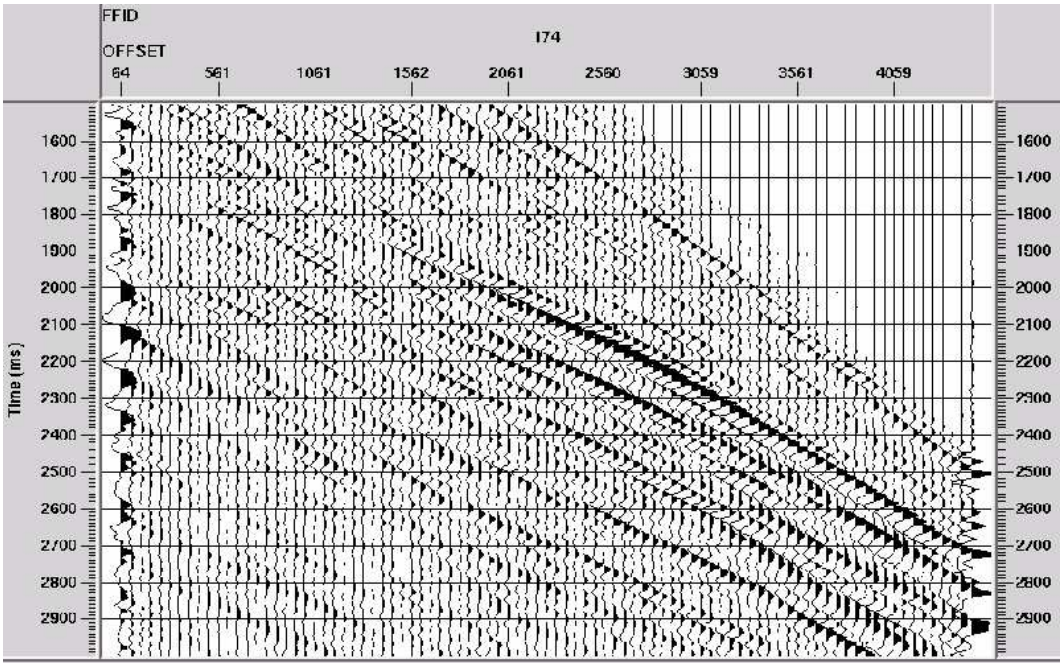

Figure 2. Gather from Figure 1 after application of F-K filtering designed to attenuate overburden noise. The target event marked in Figure 1 is clearly visible between 1500 m and 4500 m.

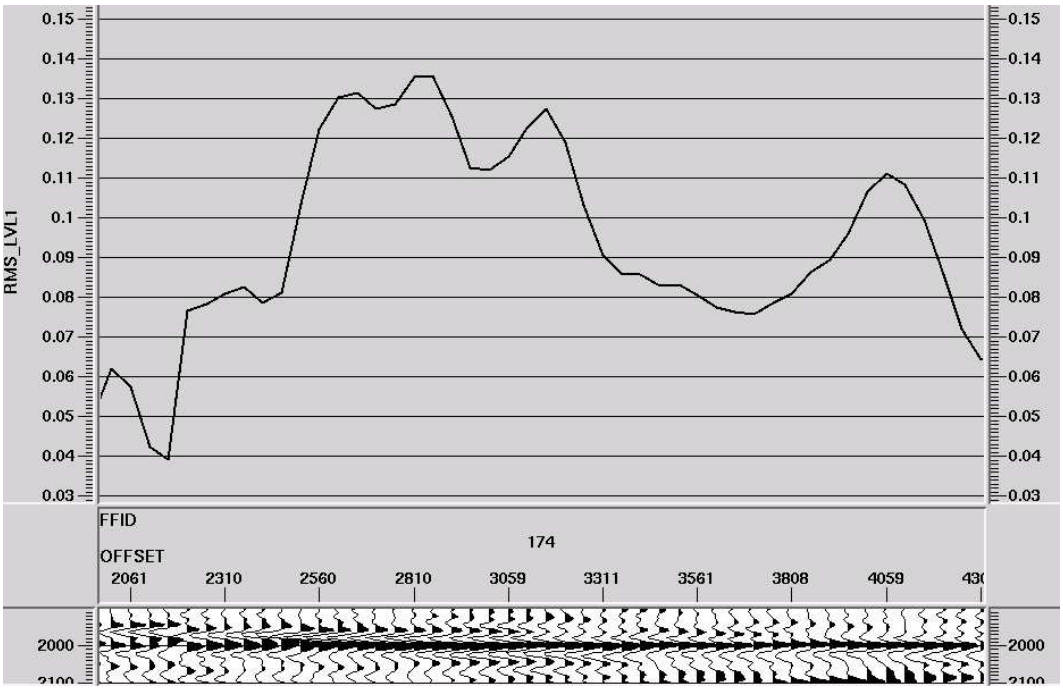

Figure 3. Estimated RMS amplitude of the target event from Figures 1 and 2 computed in a 50 ms window after F-K filtering. The offset of the fastest amplitude increase, which we interpret as corresponding to the critical-angle reflection, is near the 4 km mark. The windowed section on the bottom shows the flattened target event.

the critical offset (see below), which is close to 4 km (Figure 3). This value is in good agreement with an independent prediction of the critical offset made using borehole data (well logs) from the area. This case study supports the feasibility of critical-angle reflectometry in the presence of a significant velocity contrast at the target level.

3 CRITICAL ANGLE FOR VTI AND ORTHORHOMBIC MEDIA

We consider a plane P-wave incident upon a horizontal interface that separates two anisotropic media. If the reflecting halfspace has a higher P-wave velocity, for a certain incidence angle the group-velocity vector of the transmitted P-wave becomes horizontal. This angle, which is usually called critical, depends on the phase-velocity function and, therefore, is influenced by the velocity anisotropy. For simplicity, we assume that the reflector coincides with a symmetry plane in the reflecting halfspace, which implies that the phase-velocity vector of the transmitted wave at the critical angle is also horizontal. According to Snell's law, the horizontal slowness component of all reflected and transmitted waves should be equal to that of the incident wave, which yields

$$\frac{\sin\theta_{\rm cr}}{V_1(\theta_{\rm cr})} = \frac{1}{V_{\rm hor,2}}\,, \qquad (1)$$

where $\theta_{\rm cr}$ is the critical phase angle, $V_1(\theta)$ is the phase velocity in the incidence halfspace and $V_{\rm hor,2}$ is the horizontal phase velocity in the reflecting halfspace ($V_{\rm hor,2}$ is computed in the vertical incidence plane).

The critical angle for a particular anisotropic model can be found by solving equation 1 with the appropriate phase-velocity function $V_1(\theta)$ and the horizontal velocity $V_{\rm hor,2}$. Although this paper is mainly focused on P-waves, equation 1 remains valid for any reflected or transmitted mode. For example, the critical angle for SP-waves is obtained by simply substituting the shear-wave velocity function for $V_1(\theta)$ (see below). An alternative way of computing the critical angle is based on expressing the Christoffel equation in the incidence medium in terms of the slowness components and solving it for the horizontal slowness equal to $1/V_{\rm hor,2}$.

3.1 VTI media

Suppose both halfspaces are transversely isotropic with a vertical symmetry axis (VTI). The VTI model is azimuthally isotropic, and the critical angle has the same value in any vertical plane. To express the critical angle as a simple function of the anisotropy parameters, we employ the weak-anisotropy approximation for phase velocity linearized in the parameters ϵ and δ (Thomsen, 1986):

$$V_1(\theta) = V_{P0,1}\,(1 + \delta_1 \sin^2\theta\cos^2\theta + \epsilon_1 \sin^4\theta)\,, \qquad (2)$$

$$V_2(\theta) = V_{P0,2}\,(1 + \delta_2 \sin^2\theta \cos^2\theta + \epsilon_2 \sin^4\theta)\,, \qquad (3)$$

where the subscripts "1" and "2" denote the incident and reflecting halfspaces, respectively, and V_{P0} is the P-wave vertical velocity (it is assumed that $V_{P0,2} > V_{P0,1}$). Substituting equations 2 and 3 into equation 1, we find

$$\sin\theta_{\rm cr} = \frac{V_{P0,1}\,(1 + \delta_1 \sin^2\theta_{\rm cr} \cos^2\theta_{\rm cr} + \epsilon_1 \sin^4\theta_{\rm cr})}{V_{P0,2}\,(1+\epsilon_2)}\,. \qquad (4)$$

Within the framework of the linearized approximation, the angle $\theta_{\rm cr}$ in the terms invloving ϵ and δ can be replaced by its isotropic value $\theta_{\rm cr,is}$:

$$\sin\theta_{\rm cr,is} = \frac{V_{P0,1}}{V_{P0,2}} = n\,. \qquad (5)$$

Then the right-hand side of equation 4 no longer contains the unknown critical angle:

$$\sin\theta_{\rm cr} = \frac{V_{P0,1}\,[1 + \delta_1 n^2(1-n^2) + \epsilon_1 n^4]}{V_{P0,2}\,(1+\epsilon_2)}\,. \qquad (6)$$

Further linearization in ϵ_2 gives

$$\sin\theta_{\rm cr} = n\left[1 - \epsilon_2 + \delta_1 n^2 + (\epsilon_1 - \delta_1) n^4\right]\,. \qquad (7)$$

Since the vertical-velocity ratio $n < 1$, the contribution of anisotropy to the critical angle is controlled primarily by the parameter ϵ_2 responsible for the horizontal P-wave velocity in the reflecting halfspace.

If the incidence medium is anisotropic, the critical offset is determined by the critical group (ray) angle $\psi_{\rm cr}$, which can be computed from $\theta_{\rm cr}$ using the well-known group-velocity equations for VTI media. In the weak-anisotropy approximation (Tsvankin, 2005),

$$\psi_{\rm cr} = \theta_{\rm cr} + [\delta_1 + 2(\epsilon_1 - \delta_1)\sin^2\theta_{\rm cr}]\,\sin 2\theta_{\rm cr}\,. \qquad (8)$$

3.2 Orthorhombic media

Many naturally fractured reservoirs are believed to possess orthorhombic symmetry in the long-wavelength limit (Bakulin et al., 2000; Grechka and Kachanov, 2005). Note that most existing parameter-estimation methods for orthorhombic media rely on multicomponent data (e.g., Grechka et al., 2005), which are not acquired in the bulk of seismic surveys.

Suppose a horizontal interface separates two orthorhombic media with the same orientation of the symmetry planes, which are assumed to be aligned with the coordinate planes. Then the reflector coincides with the horizontal symmetry plane $[x_1, x_2]$, and the critically refracted ray corresponds to a horizontal slowness vector. For this model, equation 7 remains entirely valid in the vertical symmetry planes ($[x_1, x_3]$ and $[x_2, x_3]$), if ϵ and δ are replaced by the corresponding anisotropy parameters defined in Tsvankin (1997a, 2005). For example, the critical angle in the $[x_1, x_3]$-plane can be written as

$$\begin{aligned}\sin\theta_{\rm cr}\,(\phi = 0^\circ) \;&=\; n\,[1 - \epsilon_2^{(2)} + \delta_1^{(2)}\, n^2 \\ &\quad + (\epsilon_1^{(2)} - \delta_1^{(2)})\, n^4]\,, \end{aligned} \qquad (9)$$

where ϕ is the azimuth from the x_1-axis, and $\epsilon^{(2)}$ and $\delta^{(2)}$ are the anisotropy parameters defined in the $[x_1, x_3]$-plane. Using the parameters $\epsilon^{(1)}$ and $\delta^{(1)}$ instead of $\epsilon^{(2)}$ and $\delta^{(2)}$ in equation 9 yields the critical angle in the $[x_2, x_3]$ symmetry plane.

In the weak-anisotropy limit, the kinematic analogy between orthorhombic and VTI media remains valid for 2D P-wave propagation even outside the symmetry planes, if the parameters ϵ and δ are expressed as the following functions of azimuth (Tsvankin, 1997a, 2005):

$$\delta(\phi) = \delta^{(1)} \sin^2\phi \,+\, \delta^{(2)} \cos^2\phi\,, \qquad (10)$$

$$\begin{aligned}\epsilon(\phi) \;&=\; \epsilon^{(1)} \sin^4\phi + \epsilon^{(2)} \cos^4\phi \\ &\quad + (2\epsilon^{(2)} + \delta^{(3)}) \sin^2\phi \cos^2\phi\,; \end{aligned} \qquad (11)$$

the parameter $\delta^{(3)}$ is defined in the horizontal plane. Substituting $\delta(\phi)$ and $\epsilon(\phi)$ from equations 10 and 11 into equation 7, we obtain the P-wave critical angle for an arbitrary azimuth ϕ:

$$\begin{aligned}\sin\theta_{\rm cr}(\phi) \;&=\; n\,\{1 - \epsilon_2(\phi) + \delta_1(\phi)\, n^2 \\ &\quad + [\epsilon_1(\phi) - \delta_1(\phi)]\, n^4\}\,. \end{aligned} \qquad (12)$$

3.3 Numerical example

The magnitude of the azimuthal variation of the critical angle for HTI (transversely isotropic with a horizontal symmetry axis) and orthorhombic media is illustrated in Figure 4. For all three models, the reflecting layer (layer 2) is assumed to be isotropic, while the incidence medium (layer 1) has three different anisotropic symmetries (see Table 1). When layer 1 is VTI (model M1), the critical angle is constant for all azimuths, although it is different from the isotropic value $\theta_{\rm cr,is} = \sin^{-1} n$. Despite small-to-moderate values of the anisotropy parameters in the HTI (M2) and orthorhombic (M3) models, the azimuthal variation of the critical angle for them is substantial. The difference between the values of $\theta_{\rm cr}$ in the vertical symmetry planes can reach 5–7°. Such variations in the critical angle for deep interfaces would change the critical offset by hundreds of meters, which should be detectable on AVO plots similar to the one in Figure 3. Application of this method requires acquisition of long-offset, wide-azimuth data with a sufficiently high signal-to-noise ratio at near-critical offsets. At a minimum, it is necessary to acquire two orthogonal 2D lines in the symmetry planes, whose azimuths have to be determined in advance.

3.4 Critical angles for mode-converted and shear waves

Here, the discussion is restricted to VTI media and symmetry planes of orthorhombic media. Analytic description of shear waves outside symmetry planes of azimuthally anisotropic media is much more complicated

	$\epsilon^{(1)}$	$\epsilon^{(2)}$	$\delta^{(1)}$	$\delta^{(2)}$	$\delta^{(3)}$	V_{P0}(m/s)	V_{S0}(m/s)
M1 (VTI, layer 1)	0.15	0.15	0.1	0.1	0	2100	1200
M2 (HTI, layer 1)	0	-0.15	0	-0.1	0.35	2100	1200
M3 (ORTH, layer 1)	0.33	0.26	0.08	-0.08	-0.1	2100	1200
M4 (ORTH, layer 2)	0.1	0.2	0	0	-0.24	2800	1200

Table 1. Model parameters used in the numerical tests. For models M1–M3, the reflecting layer (layer 2) is isotropic with a P-wave velocity of 2800 m/s. The parameters of the HTI model are computed using the results of Tsvankin (1997b).

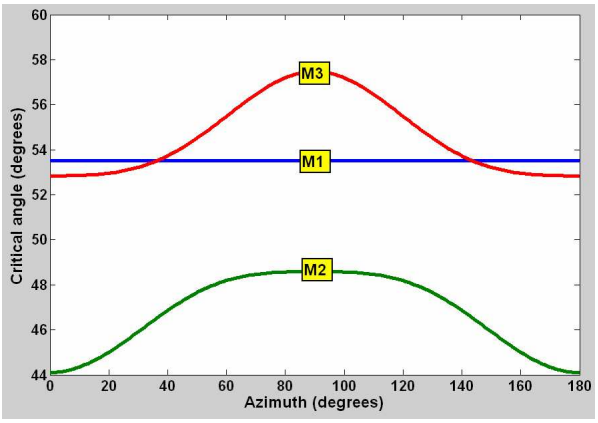

Figure 4. Critical angle of P-waves computed as a function of azimuth from equation 12. The parameters of models M1, M2, and M3 are listed in Table 1. The azimuthal anisotropy of the top (incidence) layer in models M2 and M3 causes a noticeable variation of the critical angle with azimuth.

and cannot be based on the analogy with vertical transverse isotropy. Equation 7 can be adapted for mode-converted SP-waves by applying the "substitution rule" described by Tsvankin (2005). To obtain any kinematic signature of SV-waves in the weak-anisotropy approximation from the corresponding P-wave expression, V_{P0} has to be replaced with V_{S0}, δ with the SV-wave velocity parameter $\sigma \equiv (V_{P0}^2/V_{S0}^2)\,(\epsilon - \delta)$, and ϵ set to zero.

Using this recipe, the critical angle for the SS (i.e., SVSV) transmission into the high-velocity halfspace can be found from equation 7 as

$$\sin\theta_{\rm cr,SS} = n_{\rm SS}\left[1 + \sigma_1\, n_{\rm SS}^2 - \sigma_1\, n_{\rm SS}^4\right], \qquad (13)$$

where $n_{\rm SS} \equiv V_{S0,1}/V_{S0,2}$.

Similarly, for the S-to-P (i.e., SV-to-P) transmission we have:

$$\sin\theta_{\rm cr,SP2} = n_{\rm SP2}\left[1 - \epsilon_2 + \sigma_1\, n_{\rm SP2}^2 - \sigma_1\, n_{\rm SP2}^4\right]; \qquad (14)$$

$n_{\rm SP2} \equiv V_{S0,1}/V_{P0,2}$.

For the S-to-P reflection in the incidence layer,

$$\sin\theta_{\rm cr,SP1} = n_{\rm SP1}\left[1 - \epsilon_1 + \sigma_1\, n_{\rm SP1}^2 - \sigma_1\, n_{\rm SP1}^4\right]; \qquad (15)$$

$n_{\rm SP1} \equiv V_{S0,1}/V_{P0,1}$.

Equations 13–15 remain valid for SV-waves in the vertical symmetry planes of orthorhombic media. The shear-wave critical angles can be identified from the corresponding amplitude anomalies of the reflected SS-wave. Note that the accuracy of the weak-anisotropy approximation for SV-waves usually is much lower than for P-waves because of the relatively large values of the parameter σ (Tsvankin, 2005).

In the untypical case of an extremely strong velocity contrast, the SV-wave velocity in the reflecting layer can be higher than the P-wave velocity in the incidence medium. Then application of the substitution rule yields

$$\sin\theta_{\rm cr,PS} = n_{\rm PS}\left[1 + \delta_1\, n_{\rm PS}^2 + (\epsilon_1 - \delta_1)\, n_{\rm PS}^4\right]; \qquad (16)$$

$n_{\rm PS} \equiv V_{P0,1}/V_{S0,2}$. If the vertical-velocity ratios are known, the critical angle of PS-waves provides a relationship between the parameters ϵ_1 and δ_1.

It is also important to notice that the PS-wave reflection coefficient has a peak corresponding to the critical PP reflection. Therefore, PS-wave amplitude analysis can help to get a more reliable estimate of the critical angle of PP-waves (Mehdizadeh et al., 2005).

4 WHAT CAN BE DETERMINED FROM THE CRITICAL ANGLE?

The analytic results in the previous section indicate that measurements of the critical angle contain valuable information for anisotropic parameter estimation. Here, we explore the parameter-estimation issues in more detail for both VTI and orthorhombic media.

4.1 VTI media

If the vertical-velocity ratios have been determined, for example, from borehole data, an estimate of the P-wave critical angle can be used to constrain the parameters ϵ and δ. In the simplest case of a VTI layer beneath an isotropic overburden, the angle $\theta_{\rm cr}$ depends just on ϵ_2 - the parameter responsible for the horizontal velocity in the reflecting medium (equations 1 and 7):

$$\epsilon_2 = \frac{1}{2}\left(\frac{n^2}{\sin^2\theta_{\rm cr}} - 1\right) \approx 1 - \frac{\sin\theta_{\rm cr}}{n}. \qquad (17)$$

If the reflecting layer is isotropic, while the overburden is VTI, there are two unknowns (ϵ_1 and δ_1) in equation 7, and this ambiguity cannot be resolved without additional information. For the general VTI/VTI model, measurement of the critical angle provides a relationship between the parameters ϵ_1, δ_1, and ϵ_2. Since equation 7 represents a linearized approximation, more accurate estimates of the anisotropy parameters can be obtained by solving equation 1 with the exact velocity function.

4.2 Orthorhombic media

In the azimuthal AVO analysis, the best-constrained parameter is the difference between the AVO gradients in the vertical symmetry planes (e.g., Rüger, 2001). Likewise, the critical-angle reflectometry can provide an estimate of the difference $\Delta(\sin\theta_{\rm cr})$ between the symmetry-plane critical angles. As follows from equation 12,

$$\begin{aligned}\Delta(\sin\theta_{\rm cr}) &\equiv \sin\theta_{\rm cr}(0^\circ) - \sin\theta_{\rm cr}(90^\circ)\\ &= -\,(\Delta\epsilon_2)\,n \,+\, (\Delta\delta_1)\,n^3 + (\Delta\epsilon_1 - \Delta\delta_1)\,n^5\,, \qquad (18)\end{aligned}$$

where $\Delta\delta_1 = \delta_1^{(2)} - \delta_1^{(1)}$, $\Delta\epsilon_1 = \epsilon_1^{(2)} - \epsilon_1^{(1)}$, and $\Delta\epsilon_2 = \epsilon_2^{(2)} - \epsilon_2^{(1)}$.

For the simplest case of a purely isotropic overburden, the only anisotropy parameter that influences the critical angle is ϵ_2. Then the azimuthal variation of $\sin\theta_{\rm cr}$ in equation 18 depends on the difference between the parameters $\epsilon_2^{(2)}$ and $\epsilon_2^{(1)}$:

$$\Delta\epsilon_2 = -\frac{\Delta(\sin\theta_{\rm cr})}{n}\,. \qquad (19)$$

If both layers are orthorhombic, equation 18 contains three independent anisotropic parameter combinations, which cannot be resolved without additional information. For example, if the overburden parameters have been estimated using other methods (e.g., moveout inversion), equation 18 can be used to find the difference $\Delta\epsilon_2$.

5 COMPARISON WITH REFLECTIVITY MODELING

To test the proposed method on synthetic data, we computed the wavefield for a simple model that includes an orthorhombic layer beneath an isotropic medium (Figure 5). The seismograms were generated with the anisotropic reflectivity method (Chin et al., 1984), which produces exact 3D wavefields for horizontally layered media. Our goal was to estimate the critical angle for the PP-wave reflection from the top of the orthorhombic layer (its zero-offset time is close to 950 ms).

Figure 5 shows long-spread synthetic gathers computed in two azimuthal directions 40° apart. For both azimuths, there is a weak, but clearly visible head wave splitting off from the PP-wave reflection. The separation of the head wave occurs at a larger offset for the azimuth $\phi = 40^\circ$, which is indicative of the azimuthal variation of the critical angle. Since the critical angle corresponds to a maximum of the derivative of the reflection coefficient, we associate the critical offset with the point of the fastest amplitude increase (i.e., largest slope) on the AVO curves (Figure 6). This point for $\phi = 0^\circ$ corresponds to an offset of about 1700 m, while for $\phi = 40^\circ$ it is shifted to a substantially larger offset (2000 m).

The exact critical offset for the zero-azimuth gather computed from equation 1 is 1640 m. The main reason for the small error in our estimates may be the interference between the reflected wave and the head wave. At the critical offset, the two waves essentially represent a single arrival. With the increased separation between the two waves, their interference (tuning) may result in amplitude distortions at post-critical offsets. On the whole, the modeling confirms the predicted trend of the azimuthal variation of the critical angle, although there are some discrepancies, especially for an azimuth of 90° (Figure 7).

Since the overburden in this model is isotropic, we can use the azimuthal variation of the critical angle between the symmetry planes to estimate the difference $\Delta\epsilon_2$ between the parameters $\epsilon_2^{(2)}$ and $\epsilon_2^{(1)}$ in the orthorhombic layer. Substituting the measured $\Delta(\sin\theta_{\rm cr})$ into equation 19 gives $\Delta\epsilon_2 = 0.09$, which is only slightly smaller than the exact value (0.1).

6 DISCUSSION AND CONCLUSIONS

Long-offset, wide-azimuth data can provide valuable information for building azimuthally anisotropic velocity models. Here, we introduced a method that can be called "seismic critical-angle reflectometry" because it is based on measuring the critical angle $\theta_{\rm cr}$ on reflection seismic data. When the medium above or below the reflector is anisotropic, the angle $\theta_{\rm cr}$ is strongly influenced by the anisotropy parameters.

Using the weak-anisotropy approximation, we obtained concise expressions for the critical angles of pure and mode-converted waves in VTI media and symmetry planes of orthorhombic media. For vertical transverse isotropy, the P-wave angle $\theta_{\rm cr}$ is particularly sensitive to the Thomsen parameter ϵ of the reflecting halfspace and also depends on the parameters ϵ and δ of the incidence medium. When at least one of the halfspaces is azimuthally anisotropic, the critical angle becomes azimuthally dependent. For P-waves, the angle $\theta_{\rm cr}$ in orthorhombic media is approximately described by the VTI equation with azimuthally varying parameters ϵ and δ.

Hence, the critical angle estimated from reflection data provides information about the anisotropy parameters. For a VTI layer beneath an isotropic overburden,

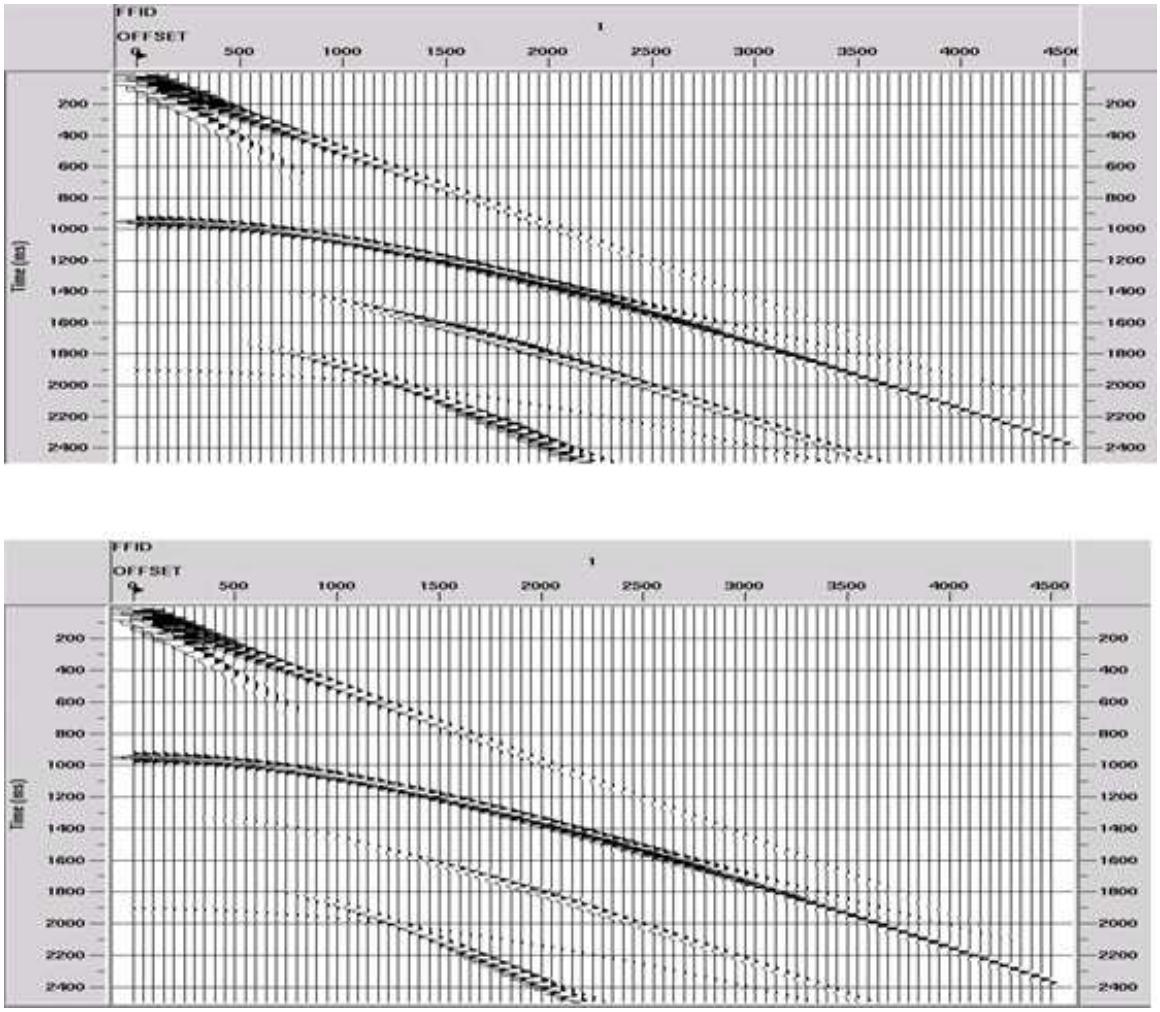

Figure 5. Synthetic seismograms of the vertical displacement for a two-layer model computed with the reflectivity method. The bottom layer is orthorhombic with the parameters of model M4 from Table 1, while the top layer is isotropic with a P-wave velocity of 2100 m/s, S-wave velocity of 1200 m/s, density of 2.5 g/cm^3, and thickness of 1000 m. The traces are plotted for a wide range of offsets in two azimuthal directions: $\phi = 0^\circ$ (top) and $\phi = 40^\circ$ (bottom). The zero-offset traveltime for the PP-wave reflection from the top of the orthorhombic layer is about 950 ms. Notice the head wave splitting off from the reflected wave at offsets between 2000 m and 2500 m.

the angle $\theta_{\rm cr}$ can be used to estimate the parameter ϵ, which is difficult to constrain from conventional-spread reflection data. When the reflecting layer is orthorhombic while the overburden is isotropic or VTI, the azimuthal variation of the critical angle is controlled by the difference between the symmetry-plane anisotropy parameters $\epsilon^{(1)}$ and $\epsilon^{(2)}$. The azimuthally dependent angle $\theta_{\rm cr}$ can also help to identify the symmetry-plane directions, which often coincide with the dominant fracture azimuths.

We verified the analytic results for the isotropic/orthorhombic interface by computing synthetic seismograms with the reflectivity method and estimating the critical angle from the point of the fastest amplitude increase on the AVO curve of the reflected wave. Although this point is somewhat shifted from the critical ray toward larger offsets, the azimuthal variation of the critical angle generally follows our prediction. We believe that the small error in our estimate of the critical angle is related primarily to the interference between the reflected and head waves. The synthetic test also shows that the extrema of the azimuthally varying function $\theta_{\rm cr}$ do not necessarily correspond to the symmetry planes, which underscores the need for a good azimuthal coverage in critical-angle reflectometry.

Application of critical-angle reflectometry to field data, however, is limited by several factors. First, generation of the critical-angle event requires a velocity increase at the top of the target layer, which is not the case

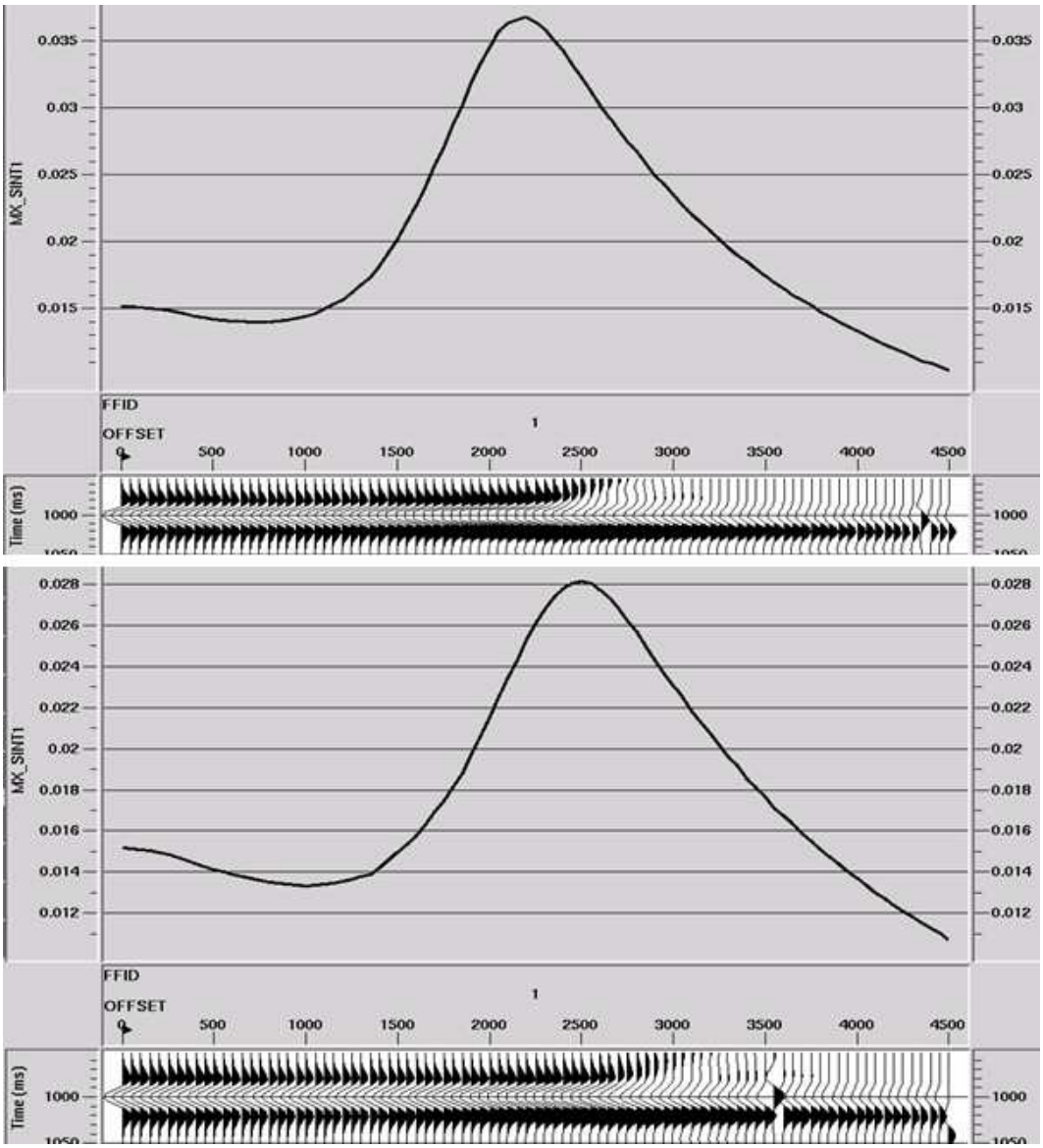

Figure 6. Amplitude of the reflected PP-wave from Figure 5 as a function of offset for the azimuths $\phi = 0°$ (top) and $\phi = 40°$ (bottom). The offset of the amplitude maximum is 2200 m for $\phi = 0°$ and 2450 m for $\phi = 40°$.

for many hydrocarbon reservoirs. Still, most carbonate and consolidated sand reservoirs have a higher velocity than that in the overburden. Second, the method has to operate on wide-azimuth, long-offset data that include the critical reflected ray from the target interface. Third, the critical-angle reflection may be obscured by the overburden noise train, which can be partially attenuated by F-K filtering and similar processing techniques. We expect that a more efficient removal of overburden noise can be achieved by model-based inversion.

Also, quantitative analysis of critical-angle measurements faces a number of serious challenges. One of them is related to the accurate detection of the critical offset on amplitude-versus-offset curves. The synthetic test discussed above shows that the point of the fastest amplitude increase does not exactly correspond to the critical offset. In addition, if the overburden is anisotropic, the AVO response of reflected waves can be strongly distorted by angle-dependent geometrical spreading (Xu et al., 2005).

Even if the critical offset has been accurately estimated from the reflection amplitude, computation of the corresponding critical angle at the target horizon requires knowledge of the overburden velocity model. An apparent variation of the critical offset can be created by reflector dip, although for mild dips of several

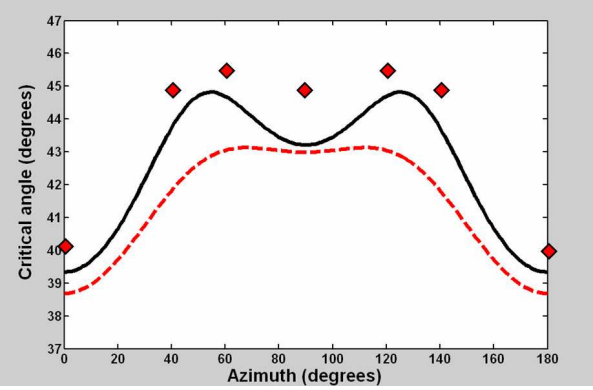

Figure 7. Variation of the critical angle with azimuth for the model from Figure 5. The diamonds mark the critical angle estimated from the reflectivity modeling, the solid line is the exact critical angle, and the dashed line is computed from thre weak-anisotropy approximation 12.

degrees such offset distortions are insignificant. Furthermore, for anisotropic media it is necessary to account for the difference between the group (ray) angle responsible for the critical offset and the phase angle of the critical ray that was analyzed in our paper. While conventional AVO analysis has to deal with the same problem, our method is more sensitive to errors in the offset-to-angle conversion because it relies on a single angle measurement for a given azimuth.

The transition from the critical offset to the critical angle may be avoided for models with a laterally homogeneous overburden. Then the amplitude of the reflected wave is convenient to treat as a function of the ray parameter (horizontal slowness), which can be estimated from the slope of the moveout curve. In the absence of lateral heterogeneity, the ray parameter at the critical offset is equal to the horizontal slowness in the high-velocity layer. For data sets with uncommonly long offsets, the horizontal velocity can also be determined from the linear moveout of the head wave. This approach gives a direct estimate of the azimuthally varying parameter ϵ in the target orthorhombic layer without knowledge of the overburden velocity model. For VTI media, the horizontal velocity can be combined with the NMO velocity to obtain the key time-processing parameter η.

On the whole, we do not envision critical-angle reflectometry as a reliable stand-alone method for anisotropic parameter estimation. Rather, it should be used in combination with existing anisotropic inversion techniques that operate with azimuthally varying traveltimes and amplitudes.

ACKNOWLEDGMENTS

We are grateful to our colleagues at the Center for Wave Phenomena (CWP), Colorado School of Mines (CSM), for useful discussions, and to Xiaoxia Xu (CSM) for her help with the reflectivity modeling and numerous suggestions. The anisotropic modeling software was developed by Dennis Corrigan (formerly of ARCO). M.L. acknowledges CSM and CWP for their hospitality during his sabbatical visit and the Norwegian Research Council (NFR) for financial support of the ROSE (Rock Seismic) project at NTNU. This work was partially supported by the Consortium Project on Seismic Inverse Methods for Complex Structures at CWP.

REFERENCES

Alkhalifah, T., 1997, Velocity analysis using nonhyperbolic moveout in transversely isotropic media: Geophysics, **62**, 1839–1854.

Alkhalifah, T., and I. Tsvankin, 1995, Velocity analysis for transversely isotropic media: Geophysics, **60**, 1550–1566.

Antich P., and S. Mehta, 1997, Ultrasound critical-angle reflectometry (UCR): A new modality for functional elastometric imaging: Physics Med. Biol., **42**, 1763–1777.

Bakulin, A., V. Grechka, and I. Tsvankin, 2000, Estimation of fracture parameters from reflection seismic data – Part II: Fractured models with orthorhombic symmetry: Geophysics, **65**, 1803–1817.

Chin, R., G. W. Hedstrom, and L. Thigpen, 1984, Matrix methods in synthetic seismograms: Geophysical Journal of the Royal Astronomical Society, **77**, 483–502.

Gray, F. D., G. Roberts, and K. J. Head, 2002, Recent advances in determination of fracture strike and crack density from P-wave seismic data: The Leading Edge, **21**, 280–285.

Grechka, V., and M. Kachanov, 2005, Multiple fractures in rocks: Effective orthotropy and seismic characterization: 75th Annual International Meeting, SEG, Expanded Abstracts, ANI 3.2.

Grechka, V., and I. Tsvankin, 1998, Feasibility of nonhyperbolic moveout inversion in transversely isotropic media: Geophysics, **63**, 957–969.

Grechka, V., and I. Tsvankin, 1999, 3-D moveout inversion in azimuthally anisotropic media with lateral velocity variation: Theory and a case study: Geophysics, **64**, 1202–1218.

Grechka, V., A. Pech, and I. Tsvankin, 2005, Parameter estimation in orthorhombic media using multicomponent wide-azimuth reflection data: Geophysics, **70**, D1–D8.

Hall, S., and J. M. Kendall, 2003, Fracture characterization at Valhall: Application of P-wave amplitude variation with offset and azimuth (AVOA) analysis to a 3-D ocean-bottom data set: Geophysics, **68**, 1150–1160.

Jílek, P., 2002, Modeling and inversion of converted-wave reflection coefficients in anisotropic media: A tool for quantitative AVO analysis: Ph.D. thesis, Colorado School of Mines.

Landrø, M., A. K. Nguyen, and H. Mehdizadeh, 2004, Time lapse refraction seismic – a tool for monitoring carbon-

ate fields?: 74th Annual International Meeting, SEG, Expanded Abstracts, 2295–2298.

Mehdizadeh, H., M. Landrø, B. A. Mythen, N. Vedanti, and R. Srivastava, 2005, Time lapse seismic analysis using long-offset PS data: 75th Annual International Meeting, SEG, Expanded Abstracts, TL 3.7.

Pankhurst, D., K. Marfurt, C. Sullivan, H. Zhou, F. Hilterman, and J. Gallaghar, 2002, Long offset AVO in a mid-continent tight gas sand reservoir: 72nd Annual International Meeting, SEG, Expanded Abstracts, 297–299.

Pech, A., and I. Tsvankin, 2004, Quartic moveout coefficient for a dipping azimuthally anisotropic layer: Geophysics, **69**, 699–707.

Rüger, A., 2001, Reflection coefficients and azimuthal AVO analysis in anisotropic media: Society of Exploration Geophysicists.

Thomsen, L., 1986, Weak elastic anisotropy: Geophysics, **51**, 1954–1966.

Toldi, J., T. Alkhalifah, P. Berthet, J. Arnaud, P. Williamson, and B. Conche, 1999, Case study of estimation of anisotropy: The Leading Edge, **18**, no. 5, 588–594.

Tsvankin, I., 1997a, Anisotropic parameters and P-wave velocity for orthorhombic media: Geophysics, **62**, 1292–1309.

Tsvankin, I., 1997b, Reflection moveout and parameter estimation for horizontal transverse isotropy: Geophysics, **62**, 614–629.

Tsvankin, I., 2005, Seismic signatures and analysis of reflection data in anisotropic media: Elsevier Science Publ. Co., Inc. (second edition).

Tsvankin, I., and V. Grechka, 2006, Developments in seismic anisotropy: Treating realistic subsurface models in imaging and fracture detection: CSEG Recorder, in print (also, this volume).

Vasconcelos, I., and I. Tsvankin, 2004, Inversion of P-wave nonhyperbolic moveout in azimuthally anisotropic media: Methodology and field-data application: 74th Annual International Meeting, SEG, Expanded Abstracts, 171–174 (also Research Report CWP–475).

Xu, X., I. Tsvankin, and A. Pech, 2005, Geometrical spreading of P-waves in horizontally layered, azimuthally anisotropic media: Geophysics, **70**, D43–D54.